Keeping it small—restricting the growth of nanocrystals

2006 J. Phys.: Condens. Matter 18 L163

(http://iopscience.iop.org/0953-8984/18/15/L01)

INSTITUTE OF PHYSICS PUBLISHING JOURNAL OF PHYSICS: CONDENSED MATTER

J. Phys.: Condens. Matter **18** (2006) L163–L170 doi:10.1088/0953-8984/18/15/L01

LETTER TO THE EDITOR

Keeping it small—restricting the growth of nanocrystals

Alan V Chadwick[1,3], Shelley L P Savin[1], Luke A O'Dell[2] and Mark E Smith[2]

[1] Functional Materials Group, School of Physical Sciences, University of Kent, Canterbury, Kent CT2 7NR, UK
[2] Department of Physics, University of Warwick, Coventry CV4 7AL, UK

E-mail: a.v.chadwick@kent.ac.uk

Received 4 February 2006
Published 30 March 2006
Online at stacks.iop.org/JPhysCM/18/L163

Abstract

A method for preventing the growth of oxide nanoparticles is presented. A second oxide phase (e.g. SiO_2) is infiltrated between the principal nanoparticles, acting as a brake on grain growth at elevated temperature. The effect of the second oxide can be significant, for example reducing the growth of SnO_2 by nearly an order of magnitude at 1000 °C. The approach is shown to be generic, being applied to six different oxides. The structures of both the nanoparticles and the even smaller secondary particles are probed by a combination of EXAFS and solid state NMR. From the Sn K-edge EXAFS it is clear that the major component SnO_2 nanoparticles are locally highly ordered, with the intensity scaling with particle size, reflecting the proportionate contribution of the lower coordinations on the surface. ^{29}Si MAS-NMR of SiO_2 particles between SnO_2 demonstrates that they are significantly more disordered than bulk SiO_2 after similar heat treatment.

1. Introduction

Properties of a diverse range of materials can be drastically changed when one or more dimensions are in the nanometre regime (Gleiter 1992, Moriarty 2001). The resulting changes in chemical (Buchachenko 2003), physical (Tjong and Chen 2004) and biological (Sarikaya *et al* 2003) behaviour, with exciting technological applications, have been of intense and ever growing interest over the last decade, and a new research area, that of *nanostructured materials*, has emerged. Nanotechnology is seen by some as '*the next industrial revolution*' (Roco 2001). This contribution is focused on one particular class of these novel materials,

[3] Author to whom any correspondence should be addressed.

namely nanocrystalline oxides, which are attracting special attention as advanced ceramics (Greil 2002), catalysts (Zhong and Maye 2001), sensors (Xu *et al* 1991) and adsorbents (Stark *et al* 1996). To maintain the key advantages in the properties exhibited by nanomaterials it is often necessary to prevent grain growth at elevated temperatures where the material will operate. This work demonstrates some novel approaches to restricting such growth and their robustness at high temperature, thereby elucidating physicochemical principles that should be widely relevant to other materials.

A specific example where nanocrystallinity is crucial to the enhanced properties is tin oxide. It has been previously shown (Davis *et al* 1998) that for copper- and iron-doped tin oxide the sensitivity to detecting CO decreases by more than three orders of magnitude as the sample is heated from 400 to 900 °C. This temperature increase caused the particle sizes to grow rapidly from ∼2 nm to greater than 50 nm; the growth is evident at temperatures as low as 400 °C. Clearly, to maintain the effectiveness of tin oxide in this gas-sensing role at all temperatures requires suppression of the particle growth, and this is a particular problem at more elevated temperatures. Several methods have been investigated with the aim of restricting grain growth, including a two-step sintering technique (Chen and Wang 2000), biomolecular capping (Torres-Martínez *et al* 1999), growing the nanocrystals in porous silica (Al-Angari 2002, Fujihara *et al* 1999), hydrothermal treatments of a sol solution (Baik *et al* 2000a, 2000b, 2000c), grafting of an organic molecule to the nanoparticle surface (Santos *et al* 2003) and grain boundary pinning via the introduction of a second phase (Al-Angari 2002, Wu *et al* 1999, Al-Angry *et al* 2003, Savin and Chadwick 2003). Although all these approaches are effective in preventing grain growth, many severely restrict access to the nanocrystalline phase, thereby negating some of the enhanced properties, such as gas sensing. In this work we report a method of restricting growth which maintains crystallite–crystallite contact and gas access that has wide applicability to metal oxides.

Wu *et al* (1999) reported the restriction of the growth of a number of nanocrystalline oxides (SnO_2, ZrO_2 and TiO_2) by treating the hydrous metal oxide gel with hexamethyldisilazane (HMDS) vapour prior to firing and formation of the nanocrystals. It was assumed that the HMDS reacted with surface hydroxyl groups and on heating to above 350 °C decomposed to form silica particles, which act as the pinning phase. This method did restrict the growth when compared to untreated samples; however, the comparison was made for a relatively low firing temperature (500 °C), where growth rates are still relatively low, and in some cases may not be sufficient to remove all traces of hydroxyl groups from the gel (e.g. ZrO_2 requires firing above 700 °C to produce the pure oxide) (Chadwick *et al* 2001). The approach of introducing silica particles clearly has much merit, and the concept is extended here by using a more controllable method of preparation, higher firing temperatures, and is shown to be applicable to a wide range of oxides.

2. Experimental section

2.1. Materials

Tin oxide and zirconium oxide were prepared by dissolving $SnCl_4{\cdot}5H_2O$ or $ZrOCl_2{\cdot}8H_2O$ (Aldrich Chemical Co.), respectively, in the minimum amount of water and adding ammonia (BDH) drop wise, with stirring, until the solutions gelled. The white solid was then washed remove chloride ions and dried at 60 °C overnight. SnO_2–SiO_2 and ZrO_2–SiO_2 (15% by weight) were prepared by mixing an aqueous solution of the respective chloride salt with an ethanolic solution of tetraethylorthosilicate (TEOS, Aldrich Chemical Co.) and stirring for 1 h. Ammonia was added drop wise, with stirring, until the solutions gelled. The white solid

was then washed to remove chloride ions and dried at 60 °C overnight. Magnesium oxide and titanium oxide were prepared by adding water, with stirring, to magnesium methoxide solution (6–10% in methanol, Aldrich Chemical Co.) or to titanium *iso*-propoxide (Aldrich Chemical Co.), until the solutions gelled. The sample was first dried overnight in a fume cupboard and then at 80 °C until fully dry. $MgO–SiO_2$ and $TiO_2–SiO_2$ (15% by weight) were prepared by mixing for 1 h the respective metal alkoxide solution with tetraethylorthosilicate (TEOS). Water was then added, with stirring, until the solutions gelled. The samples were first dried overnight in a fume cupboard and then at 80 °C until fully dry. In each case, the dried solid was ground using a mortar and pestle and portions calcined for 1 h, in air, at 1000 °C.

Lithium niobate was prepared under nitrogen by mixing for 10 min stoichiometric quantities of lithium ethoxide (1.0 M solution in ethyl alcohol, Aldrich Chemical Co.) and niobium V ethoxide (99.95%, Aldrich Chemical Co.). $LiNbO_3–SiO_2$ (15% by weight) was prepared in the same manner but silica was incorporated by the addition of tetraethylorthosilicate with further stirring. In both cases, the sample was removed from the inert atmosphere and hydrolysed by the addition of water to form a gel. This was dried at 120 °C to form the precursor xerogel, which was calcined at 800 °C.

2.2. X-ray powder diffraction

X-ray powder diffraction patterns of the samples were collected on a conventional laboratory diffractometer, a Phillips PW1720 instrument using a Cu Kα tube operating at 35 kV and 20 mA. Particle sizes, S, were determined from the Scherrer equation (Klug and Alexander 1974), i.e.,

$$S = \frac{K\lambda}{\beta \cos\theta} \tag{1}$$

where K is a constant (0.89), β is the full-width-at-half-maximum height of the diffraction peak at angle θ, and λ is the x-ray wavelength.

2.3. Extended x-ray absorption fine structure (EXAFS)

Measurements were made on station 9.3 at the CCLRC Daresbury Synchrotron Radiation Source. The synchrotron has an electron energy of 2 GeV and the average current during the measurements was 150 mA. Sn K-edge EXAFS spectra for the powdered materials were collected at room temperature in conventional transmission mode using gas-filled ion chamber detectors. Spectra were typically collected to $k = 18$ Å^{-1} and several scans were taken to improve the signal-to-noise ratio. The data were processed in the conventional manner using the Daresbury suite of EXAFS programmes: EXCALIB, EXBACK and EXCURV98 (Binsted *et al* 1992, Binsted 1998).

2.4. Magic angle spinning NMR (MAS-NMR)

All MAS-NMR spectra were recorded using a one-pulse sequence with the Spinsight program and Chemagnetics CMX, Infinity or Infinity Plus spectrometers. The dmfit2003 programme (Massiot *et al* 2002) was used to simulate the spectra and fit the peaks. ^{29}Si spectra were obtained in a 7.05 T magnetic field (^{29}Si Larmor frequency 59.6 MHz) using a 7 mm rotor spinning at ∼3.5 kHz. They were referenced using a tetramethylsilane signal set to 0 ppm. The pulse width used was around 1.5 s, causing a tipping angle of 30°. The recycle delay was 30 s, although the average acquisition time for each sample was 24–48 h due to the relatively low

Table 1. The particle sizes of the nanocrystals with and without the addition of silica. ($^{+}$t-ZrO_2 and m-ZrO_2 are tetragonal and monoclinic phase zirconia, respectively; *a-TiO_2 and r-TiO_2 are anatase and rutile phase titania, respectively).

Oxide	Heat treatment	Particle size (nm)
Pure SnO_2	As prepared 20 °C, dried at 60 °C	2
	60 min at 1000 °C	56
SnO_2/15%SiO_2	As prepared 20 °C, dried at 60 °C	2
	60 min at 1000 °C	8
ZrO_2	As prepared 20 °C, dried at 60 °C	Amorphous
	60 min at 1000 °C	48 (m-ZrO_2)$^{+}$
ZrO_2/15%SiO_2	As prepared 20 °C, dried at 60 °C	Amorphous
	60 min at 1000 °C	10 (t-ZrO_2)$^{+}$
MgO	As prepared 20 °C, dried at 80 °C	$Mg(OH)_2$
	60 min at 1000 °C	61
MgO/15%SiO_2	As prepared 20 °C, dried at 80 °C	$Mg(OH)(OCH_3)$
	60 min at 1000 °C	11
TiO_2	60 min at 1000 °C	45 (r-TiO_2)*
TiO_2/15%SiO_2	60 min at 1000 °C	27 (a&r-TiO_2)*
$LiNbO_3$	60 min at 800 °C	201
$LiNbO_3$/15%SiO_2	60 min at 800 °C	44

abundance of the ^{29}Si isotope (4.7%) and the small amount of silica in the samples (15% by weight).

3. Results and discussion

It has been found the most reproducible and efficient method of adding silica is the introduction of tetraethylorthosilicate (TEOS) prior to the hydrolysis of either a metal alkoxide or an aqueous solution of the metal chloride. For example, alkoxides have been used to prepare MgO, TiO_2 and $LiNbO_3$, and aqueous chlorides to prepare SnO_2 and ZrO_2. The amount of silica is easily controlled by varying the volume of added TEOS. In general it appears that the addition of 15% by weight of silica is effective in restricting the growth of most oxides. A careful study of the firing was made, heating for 60 min in air at 100 °C intervals, and the results for the highest firing temperature are reported in table 1.

The XRD patterns for untreated and silica-treated SnO_2, ZrO_2 and MgO after firing for 60 min at 1000 °C are shown in figure 1. The silica-treated samples clearly show the broader peaks and the particle sizes are given in table 1. There are two other interesting features in figure 1, firstly the complete absence of any peaks due to silica, and secondly the fact that the treated ZrO_2 sample is still in the tetragonal phase. The evolution of particle size with firing temperature for the same three systems is shown in figure 2. It should be noted that the treated ZrO_2 sample did not crystallize until 800 °C. This figure emphasizes the very rapid growth above 500 °C (approximately exponential) and the effectiveness of the silica treatment.

EXAFS is another method of probing particle size and disorder in crystalline solids (Chadwick and Rush 2001), and the results for the Sn K-edge in SnO_2 are shown in figure 3. This figure presents the Fourier transform of the EXAFS and is effectively a radial distribution function around the Sn atom, for samples of known particle size. The key feature is the double peak around 3.7 Å, which is the Sn–Sn correlation, and the amplitude can be related to the average coordination number and any disorder in the crystallites. Careful analysis (Chadwick and Rush 2001, Davis *et al* 1997, Briois *et al* 1995) has shown the particles are not disordered

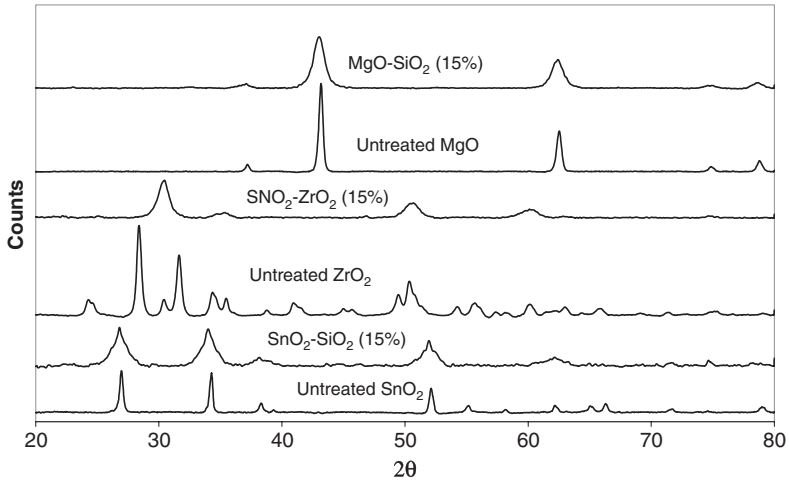

Figure 1. The x-ray diffraction patterns for various nanocrystalline oxides, with and without the addition of silica, after firing for 60 min at 1000 °C.

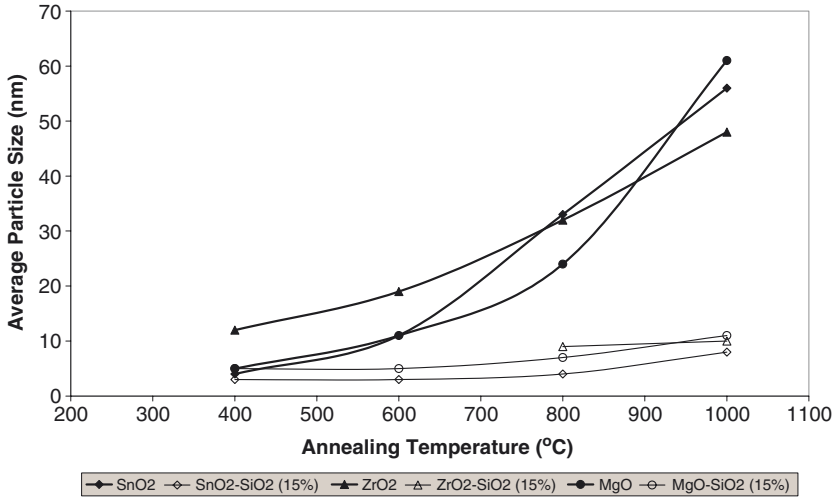

Figure 2. The particle sizes of various nanocrystalline oxides, with and without the addition of silica, after firing for 60 min at a range of temperatures.

and the amplitude can be directly correlated with particle size. Attention is drawn to the plot for the silica-treated sample that lies precisely in the position expected for the particle size.

This method of restricting the grain growth in nanocrystalline metal oxides seems to be generally applicable and effective at high temperatures. However, the mechanism by which the silica is restricting growth may not be the same for all the oxides. It is very difficult to obtain definitive information on the structural detail and distribution of the silica phase. It is clearly not a simple coating of the oxide particles by a silica film as we have shown, in the case of SnO_2 (Savin and Chadwick 2003, Savin 2003), that there is still electrical contact between the grains and the material is a very effective gas sensor. In addition, even after heating the silica-treated SnO_2 and ZrO_2 at 1200 °C there were no peaks in the XRD due to crystalline

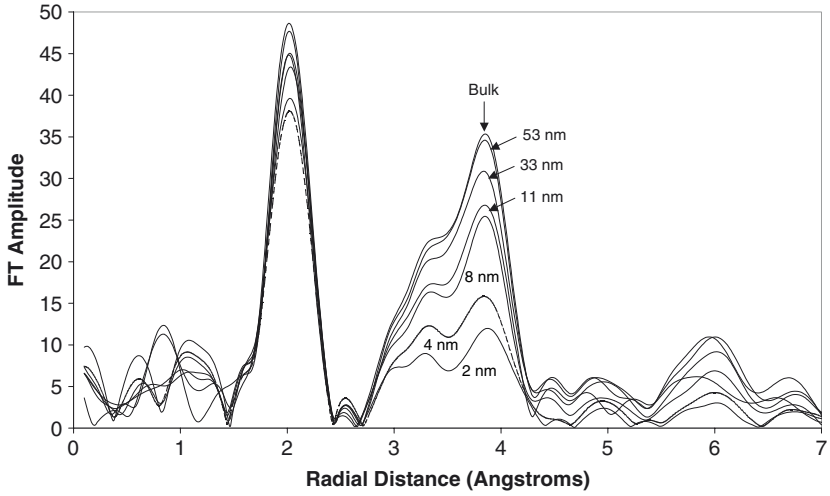

Figure 3. The Fourier transforms of the Sn K-edge EXAFS for nanocrystalline and bulk SnO_2. Included are the data for a sample with silica addition that has been fired at 1000 °C for 60 min (8 nm).

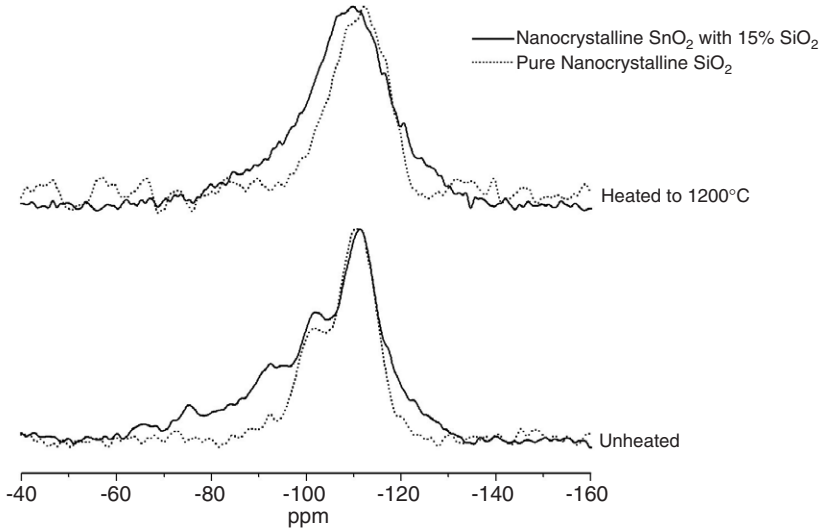

Figure 4. ^{29}Si MAS-NMR spectra of sol–gel formed SiO_2, pure and 15% with SnO_2, collected at 59.625 MHz spinning at ∼3.5 kHz with approximately 1000 scans with a 30° pulse and recycle delay of 30 s.

silica. Further evidence for the silica being in a discrete amorphous phase is the Si K-edge x-ray absorption near-edge structure (XANES), the spectra for which are characteristic of amorphous silica (Savin *et al* 2005).

Some preliminary MAS-NMR ^{29}Si results are shown in figure 4. ^{29}Si MAS-NMR is very sensitive to the atomic scale connectivity of the tetrahedral Q^n units (MacKenzie and Smith 2002) (where n is the number of bridging oxygen atoms). Figure 4 compares pure sol–gel

prepared nanocrystalline silica with the same material acting as a pinning agent for SnO_2. There are remarkable differences in the Q^n distribution between these two cases. In both unheated samples there is a full range of Q^n species present ($0 \leqslant n \leqslant 4$). However, in the silica-pinned SnO_2 sample heated to 1200 °C there are still significant amounts of $Q^{2,3}$, in addition to the expected dominant Q^4 species. This is a different atomic scale structure from the pure silica heated to 1200 °C, which implies that the interparticle confinement between SnO_2 is having a profound effect on the silica structure. It is believed at this stage that the SnO_2 nanocrystallinity is preserved by pinning of the grain boundaries (Zener pinning) by aggregates of silica.

4. Conclusions

The introduction of silica provides a simple method of preserving nanocrystallinity, and hence enhanced properties in such oxides at high temperatures should result in a very wide range of potential technological applications.

This work was funded by the EPSRC grants GR/S61881 and GR/S61898. We also thank staff at the Daresbury SRS for assistance with the EXAFS experiments.

References

Al-Angari Y 2002 *PhD Thesis* University of Kent, UK
Al-Angry Y, Savin S L P, Rammutla K E, Pooley M J, van Eck E R H and Chadwick A V 2003 *Radiat. Eff. Defects Solids* **158** 209–13
Baik N S, Sakai G, Miura N and Yamazoe N 2000a *J. Am. Ceram. Soc.* **83** 2983–7
Baik N S, Sakai G, Miura N and Yamazoe N 2000b *Sensors Actuators* B **63** 74–9
Baik N S, Sakai G, Shimanoe K, Miura K and Yamazoe N 2000c *Sensors Actuators* B **65** 97–100
Binsted N 1998 *EXCURV98* CCLRC Daresbury Laboratory computer program
Binsted N, Campbell J W, Gurman S J and Stephenson P C 1992 SERC Daresbury Program Library, Daresbury Laboratory, Warrington, Cheshire WA4 4AD, UK
Briois V, Santilli C V, Pulcinelli S H and Brito G E S 1995 *J. Non-Cryst. Solids* **191** 17–28
Buchachenko A L 2003 *Russ. Chem. Rev.* **72** 375–91
Chadwick A V, Mountjoy G, Nield V M, Poplett I J F, Smith M E, Strange J H and Tucker M G 2001 *Chem. Mater.* **13** 1219–29
Chadwick A V and Rush G E 2001 *Nanocrystalline Metals and Oxides: Selected Properties and Applications* ed P Knauth and J Schoonman (Boston: Kluwer) pp 133–64
Chen L-W and Wang X-H 2000 *Nature* **404** 168–71
Davis S R, Chadwick A V and Wright J D 1998 *J. Mater. Chem.* **8** 2065–71
Davis S R, Chadwick A V and Wright J D 1997 *J. Phys. Chem.* B **101** 9901–8
Fujihara S, Mochizuki C and Kimura T 1999 *J. Non-Cryst. Solids* **244** 267–74
Gleiter H 1992 *Adv. Mater.* **4** 474–81
Greil P 2002 *Adv. Mater.* **14** 709–16
Klug H P and Alexander L E 1974 *X-ray Diffraction Procedures* (New York: Wiley)
MacKenzie K J D and Smith M E 2002 *Multinuclear Solid State NMR of Inorganic Materials* (Oxford: Pergamon)
Massiot D, Fayon F, Capron M, King I, Le Calvé S, Alonso B, Durand J-O, Bujoli B, Gan Z and Hoatson G 2002 *Magn. Res. Chem.* **40** 70–6
Moriarty P 2001 *Rep. Prog. Phys.* **64** 297–381
Roco M C 2001 *J. Nanopart. Res.* **3** 353–60
Santos L R B, Belin S, Briois V, Santilli C V, Pulcinelli S H and Larbot A 2003 *J. Sol-Gel Sci. Technol.* **26** 171–5
Sarikaya M, Tamerler C, Jen A K Y, Schulten K and Baneyx F 2003 *Nat. Mater.* **2** 577–85
Savin S L P 2003 *PhD Thesis* University of Kent, UK
Savin S L P and Chadwick A V 2003 *Radiat. Eff. Defects Solids* **158** 73–6
Savin S L P, Chadwick A V, O'Dell L and Smith M E 2005 *Phys. Status Solidi* c **2** 661–4
Stark J V, Park D G, Lagadic I and Klabunde K J 1996 *Chem. Mater.* **8** 1904–12
Tjong S C and Chen H 2004 *Mater. Sci. Eng.* R **45** 1–88

Torres-Martínez C L, Nguyen L, Kho R, Bae W, Bozhilov K, Klimov V and Mehra R K 1999 *Nanotechnology* **10** 340–54
Wu N-L, Wang S-Y and Rusakova I A 1999 *Science* **285** 1375–7
Xu C, Tamaki J, Miura N and Yamazoe N 1991 *Sensors Actuators* B **3** 147–55
Zhong C J and Maye M M 2001 *Adv. Mater.* **13** 1507–11